Heliyon

Resistive drift instabilities for thermal and non-thermal electron distributions in electron-ion plasma

Umer Rehman [a,b,*]

[a] *CAS Key Laboratory of Geospace Environment, University of Science and Technology of China, Hefei, 230026, PR China*

[b] *Department of Engineering and Applied Physics, University of Science and Technology of China, Hefei, 230026, PR China*

* Corresponding author.
E-mail address: umer@mail.ustc.edu.cn (U. Rehman).

Abstract

Local dispersion relations for resistive drift mode in a nonuniform magnetize plasma are derived for thermal and non-thermal distribution of electrons. The coupled mode equations are obtained by using Braginskii's transport equations for ions and electrons with thermal as well as non-thermal (Cairns and kappa) distribution for electrons. The dispersion relations are then analyzed both analytically as well as numerically for all distributions. It is found that growth rate is highest for Maxwellian, Intermediate for kappa and lowest for Cairns distribution. It has been found that increasing values of Γ (which estimate population of non-thermal electrons) for Cairn distributed electrons are able to stabilize the mode. Furthermore, increasing the values of κ (which is spectral index) for the kappa distributed electrons have destabilizing effects on the mode. The result might be useful in the interpretation of electromagnetic fluctuations in nonuniform magneto-plasma in which resistivity is a key element in calculation of drift instabilities in the presence of thermal or nonthermal electron distributions, such systems are extensively observed in laboratory as well as space plasma.

Keyword: Plasma physics

1. Introduction

Initially the resistive drift instability in potential approximation was described by Moiseev and Sagdeev [1]. Later, Mikhailovskii [2] presented a comprehensive electromagnetic theory of this instability. Furthermore, he extended the electromagnetic fluid model to kinetic estimations with use of model collisional operator [3]. Recently, Mirnov et al. [4] presented analytical and numerical results of this instability by following Mikhailovskii work [2, 3]. Inclusion of finite resistivity in the model is the key element in calculations of resistive drift instability, if the electrons are free to move along magnetic field to cancel the charge separation, there will be stable drift wave. When the electron motion is delayed due to collision of electron with ion, a phase shift appears that results in instability. The data base on observations of space plasmas have shown widespread ion and electron populations and away from their thermal equilibrium [5, 6, 7, 8, 9, 10, 11, 12, 13]. The main motivation factor for this work is to study such instability for thermal and non-thermal distribution of electrons for space plasma.

There are many space plasma environments like ionosphere, solar wind, astronomical objects, interstellar medium, magnetosphere of Earth and other planetary environments, where non-thermal distribution functions are very common [14, 15, 16, 17]. Cairns *et al.* [15] proposed highly non-Maxwellian distribution profile, which has been observed to exist in space plasma [16, 17, 18]. There is another commonly employed distribution profile is kappa distribution [14], characterized by the parameter κ. Both distributions have been applied to study many types of acoustic solitons. For instance, Cairns *et al.* [15] demonstrated that the nature of ion-acoustic solitary structures could change due to presence of non-Maxwellian electron distribution and camp up with an explanation of structures observed by the Freja and Viking satellites [19, 20]. Mamun [21] have applied the Cairns distributed electrons and investigated the effect of ion temperature on ion acoustic solitary waves. The supra-thermal particles are well described by κ-distribution. Vasyliunas [14] used κ-distribution to fit OGO 1 and OGO 2 solar wind data. Since then, it has been extensively used by many scientists [22, 23]. Khan et al [24]. investigated dispersion properties of ion-acoustic plasma vortices. Later, Rehman et. al [25]. discussed the orbital angular momentum states of twisted electrons acoustic waves with double kappa distribution for electrons. Recently, Usman *et. al* [26] investigated Unique features of parallel whistler instability using Cairns distribution. Batool *et al.* [27] demonstrated the effect of nonthermal electron distribution on ITG driven drift instabilities They found significant modification in ITG driven drift mode due to presence of non-thermal distributed electrons.

In this paper, resistive drift instabilities are demonstrated by using Maxwellian and non-Maxwellian distribution of electrons. Well known two types of non-Maxwellian

distributions have been used i.e. Cairns and kappa. Three dispersion relations have been derived and solved numerically for space plasma physical parameters. The effect of Maxwellian, Cairns and kappa distributed electron on the mode have also been pointed out. The limiting case has been discussed, so that one can retrieve the well know results of Ref. [1, 2, 3, 28].

The rest of manuscript is arranged in the following manner. Section 2 is allocated for the theory of the electromagnetic perturbation. In Section 3 calculations have been carried out, in order to obtain the dispersion relation. Section 4 contains results of the present investigation.

2. Theory

Let us assume a nonuniform plasma composed of electrons and ions, placed in nonuniform externally applied magnetic field B along z-direction in Cartesian coordinate system. The equilibrium number density gradient $dn_0(x)/dx$ is along x-axis. Assuming hot electrons and cold ions. The mathematical model for dynamics of plasma read as,

$$m_i n \left(\frac{\partial v_i}{\partial t} \right) = en(E + v_i \times B), \tag{1}$$

$$m_e n \left(\frac{\partial v_e}{\partial t} \right) = -en(E + v_e \times B) - \nabla p_e - n^2 e^2 \eta (v_e - v_i), \tag{2}$$

$$\frac{\partial n_j}{\partial t} + \nabla_\perp \cdot \left(n v_{j\perp} \right) + \frac{\partial}{\partial z} \left(n v_{jz} \right) = 0, \tag{3}$$

$$\nabla \times B = \frac{4\pi}{c} j. \tag{4}$$

Eqs. (1) and (2) are equation of motion for ion and electron fluid respectively, Eq. (3) is continuity equation for *jth* specie, where j (*=e and i*) represents e for electron and i for ion, whereas Eq. (4) is Ampere's law. To close system of equations use equation of state $p_e = n_e T_e$ and electron density for thermal and non-thermal electron distributions as,

$$n_e = n_0 \exp(\phi), \tag{5}$$

$$n_e = n_0 \left(1 - q\phi + q\phi^2 \right) \exp(\phi), \tag{6}$$

$$n_e = n_0 (1 - \phi/\kappa)^{-\kappa+1/2}, \tag{7}$$

where $\phi = e\varphi/T_e$, Eq. (5) is for thermal distribution whereas Eqs. (6) and (7) are for non-thermal distributions (Cairns and kappa respectively), n_0 is equilibrium

density of electrons and q is given by $4\Gamma/(1 + 3\Gamma)$, here Γ is parameter which determines the population of non-thermal electrons and κ is real parameter giving deviation from thermal distribution.

3. Calculation

Considering quasi-neutrality condition i.e. $n_{e0} = n_{i0} = n_0$ and applying drift-approximation $|\partial/\partial t| \ll \omega_{ic} \ll \omega_{ec}(= eB_0/m_jc)$, where ω_{jc} is the cyclotron-frequency, e is the magnitude of electronic charge, m_j is mass of specie and c is the speed of light, from Eqs. (1) and (2) linearized perpendicular (to equilibrium magnetic field) component of ion and electron fluid velocity is,

$$v_{i1\perp} = \frac{c}{B_0}(\widehat{z} \times \nabla_\perp \phi) - \frac{m_i c}{eB_0^2}\left(\frac{\partial}{\partial t}\nabla_\perp \phi\right),$$ (8)

$$v_{e1\perp} = \frac{c}{B_0}(\widehat{z} \times \nabla_\perp \phi) - \frac{T_e c}{en_0 B_0}(\widehat{z} \times \nabla_\perp n_{e1}).$$ (9)

Ion total drift velocity is composed of ExB drift and polarization drift as given in Eq. (8) while electron drift composed of total drift velocity due to ExB drift and diamagnetic drift as given in Eq. (9), electric field used in term of scaler potential ϕ as $E = -\nabla\phi - 1/c(\partial A_z/\partial t)$, where A_z is vector potential exist along z-direction. The equilibrium or zero order quantities are labeled by the subscripts zero while first order perturbed quantities are represented by the subscripts 1 as given in Eqs. (8) and (9).

After linearization and doing simple algebraic steps by putting linearized perpendicular and parallel components of electron and ion velocities into continuity Eq. (3) for each respective specie and assuming quasi-neutrality condition $n_{e1} = n_{i1}$, obtain,

$$\left(\frac{\partial}{\partial t} + \frac{T_e c}{en_o B_0}\frac{dn_o}{dx}\frac{\partial}{\partial y}\right)\left(\frac{T_e c}{en_0 B_0}\frac{dn_0}{dx} + \frac{T_e c m_i}{e^2 B_0^2}\frac{\partial^2}{\partial t^2}\nabla_\perp^2 + \frac{T_e}{m_i}\frac{\partial^2}{\partial z^2} + \frac{T_e c}{m_i}\frac{\partial}{\partial z}\frac{\partial A_z}{\partial t}\right)n_{e1}$$
$$-\frac{T_e c}{en_o B_0}\frac{\partial}{\partial t}\frac{dn_o}{dx}\frac{\partial}{\partial y}\phi + \frac{T_e}{n_0 e^2 \eta}\frac{\partial^2}{\partial z^2}\frac{\partial^2 \phi}{\partial t^2} + \frac{T_e}{cn_0 e^2 \eta}\frac{\partial}{\partial z}\frac{\partial A_z}{\partial t}\frac{\partial^2 \phi}{\partial t^2} = 0.$$ (10)

Electrons are assumed to be inertia-less to get above relation (10). Using magnetic field in terms of vector potential Eq. (4) yields,

$$\nabla_\perp^2 A_z = -\frac{4\pi}{c}(env_{i1z} - env_{e1z}),$$ (11)

putting z-components of velocities in above equation give,

$$\left(\nabla_\perp^2 - \frac{4\pi e^2 n_o}{m_i c^2} - \frac{4\pi}{c^2 \eta}\frac{\partial}{\partial t}\right)\frac{\partial A_z}{\partial t} = \left(\frac{4\pi e^2 n_0}{m_i c} + \frac{4\pi}{c^2 \eta}\frac{\partial}{\partial t}\right)\frac{\partial \phi}{\partial z}, \tag{12}$$

combining Eqs. (11) and (12),

$$\left(\frac{\partial}{\partial t} + v_{*e}^n \frac{\partial}{\partial y}\right)\left(\rho_s^2 \frac{\partial^2}{\partial t^2}\nabla_\perp^2 + c_s^2 \frac{\partial^2}{\partial z^2} + \left(\frac{c_s^2 d_i^4 \frac{\partial^2}{\partial z^2} + c_s^2 \frac{d_i^2}{D_m}\frac{\partial}{\partial t}\frac{\partial^2}{\partial z^2}}{d_i^2 \nabla_\perp^2 - 1 - \frac{d_i^2}{D_m}\frac{\partial}{\partial t}}\right)\right)n_{e1}$$

$$+ c_s^2 \frac{d_i^2}{D_m}\frac{\partial^2}{\partial z^2}\frac{\partial^2}{\partial t^2}\phi + \left(\frac{c_s^2 \frac{d_i^2}{D_m}\frac{\partial^2 \partial^2}{\partial z^2 \partial t^2} + c_s^2 \frac{d_i^4}{D_m^2}\frac{\partial^3}{\partial t^3}\frac{\partial^2}{\partial z^2}}{d_i^2 \nabla_\perp^2 - 1 - \frac{d_i^2}{D_m}\frac{\partial}{\partial t}}\right)\phi = 0, \tag{13}$$

where defining plasma parameters as $v_{*e}^n = (T_e c / B_0 e n_0)dn_0/dx$ is diamagnetic drift velocity of electron, $d_i = c/\omega_{pi}$ is ion skin depth (here c is speed of light and, $\omega_{pi} = (4\pi n_0 e^2/m_i)^{1/2}$ is plasma frequency of ion), $\beta = 4\pi n_0 T_e/B_0^2$ is plasma beta (ration of kinetic pressure to magnetic pressure), $c_s^2 = T_e/m_i$ is the speed of sound, $\rho_s = \sqrt{\beta}d_i$ ion-sound radius and $D_m = \eta c^2/4\pi$ is the resistive diffusion co-efficient in terms of resistivity η.

4. Results & discussion

To get the local linear dispersion relation for Maxwellian distributed electrons, using linearize Boltzmann distribution into Eq. (13). Furthermore, assuming that the scalar potential ϕ is proportional to $\exp[-i(\omega t - \mathbf{k}.\mathbf{r})]$, where ω is the angular frequency of wave, $\mathbf{k}$ is the wave-vector. The dimensionless form of dispersion relations can be written as,

$$\left(\tilde{\omega}\left(\tilde{\omega} + \frac{i\beta k_\perp^2}{S}\right) - \tilde{\omega}_{*e}^n\left(\tilde{\omega} + \frac{i\beta k_\perp^2}{S}\right)\right)\left(\rho_s^2 k_\perp^2 \tilde{\omega}^2\left(\tilde{\omega} + \frac{i\beta k_\perp^2}{S}\right) - k_z^2\left(\tilde{\omega} + \frac{i\beta k_\perp^2}{S}\right)\right.$$

$$\left. + \frac{i\beta k_\perp^2}{S} + \beta k_z^2 \tilde{\omega}\right) + \beta k_z^2 \tilde{\omega}^2\left(\tilde{\omega} + \frac{i\beta k_\perp^2}{S}\right) = 0. \tag{14}$$

Dispersion relations for non-Maxwellian distributed electrons i.e. Cairn distribution can be obtained by using linearize form of Eq. (6) into Eq. (13), and get,

$$\left(\tilde{\omega}\left(\tilde{\omega} + \frac{i\beta k_\perp^2}{S}\right) - \tilde{\omega}_{*e}^n\left(\tilde{\omega} + \frac{i\beta k_\perp^2}{S}\right)\right)\left(\rho_s^2 k_\perp^2 \tilde{\omega}^2\left(\tilde{\omega} + \frac{i\beta k_\perp^2}{S}\right)\right.$$

$$\left. - k_z^2\left(\tilde{\omega} + \frac{i\beta k_\perp^2}{S}\right) + \frac{i\beta k_\perp^2}{S} + \beta k_z^2 \tilde{\omega}\right)(1-q) + \beta k_z^2 \tilde{\omega}^2\left(\tilde{\omega} + \frac{i\beta k_\perp^2}{S}\right) = 0, \tag{15}$$

and similarly, dispersion relation for kappa distributed electrons can be obtained by using linearize form of Eq. (7) into Eq. (13),

$$\left(\tilde{\omega}\left(\tilde{\omega}+\frac{i\beta k_\perp^2}{S}\right)-\tilde{\omega}_{*e}^n\left(\tilde{\omega}+\frac{i\beta k_\perp^2}{S}\right)\right)\left(\rho_s^2 k_\perp^2 \tilde{\omega}^2\left(\tilde{\omega}+\frac{i\beta k_\perp^2}{S}\right)-k_z^2\left(\tilde{\omega}+\frac{i\beta k_\perp^2}{S}\right)\right)$$

$$+\frac{i\beta k_\perp^2}{S}+\beta k_z^2 \tilde{\omega}\right)\left(\frac{\kappa-\frac{1}{2}}{\kappa}\right)+\beta k_z^2 \tilde{\omega}^2\left(\tilde{\omega}+\frac{i\beta k_\perp^2}{S}\right)=0,$$

$$\text{(16)}$$

where dimensionless variables, $\tilde{\omega}=\omega\tau_A$, $S=\tau_\eta/\tau_A$, $\beta=c_s^2/v_A^2$ and $\tilde{\omega}_{*e}^n=\beta d_i k_\perp/L_n$ are used, here $L_n\to L_n/L$ is the dimensionless density gradient scale length and $d_i\to d_i/L$ is dimensionless ion skin depth, while $\tau_\eta=L/D_m$ and τ_A are resistive diffusion and Alfven time scales respectively.

Eqs. (14), (15), and (16) are resistive drift mode for thermal, Cairns and kappa distributed electrons respectively. The term $(1-q)$ determines the effect of Cairns distribution of electrons on mode and the term $((\kappa-1/2)/\kappa)$ expresses the effect of kappa distributed electrons on linear propagation of drift mode. In the limit $S\to\infty$ and considering the electrostatic perturbation $(\tilde{\omega}\ll k_z L)$ case as discussed in Ref. [1, 2, 3], well know electrostatic drift mode can be retrieve for Maxwellian distributed electrons [2, 28], Further assumption to the uniform plasma with $\tilde{\omega}_{*e}^n=0$ yields basic modes of uniform plasma as discussed in Ref. [28].

By choosing typical physical parameters found in space plasma, some numerical results are presented for Maxwellian as well as non-Maxwellian plasma. Fig. 1 demonstrates the comparison of imaginary part of the mode for Eqs. (14) and (15) and Eq. (16) i.e. Maxwellian, Cairns and kappa distributed electrons respectively against the parallel wave with Lindquist number $S=10^7, d_i=0.1, \beta=0.5, T_e=10^5 eV$, $L_n/L=2$ and $d_i/L=0.1$.

Fig. 1 shows the highest unstable mode of the spectrum for all distributions occur at same fixed k_z and the growth rate is highest for Maxwellian, Intermediate for kappa and lowest for Cairns distributions.
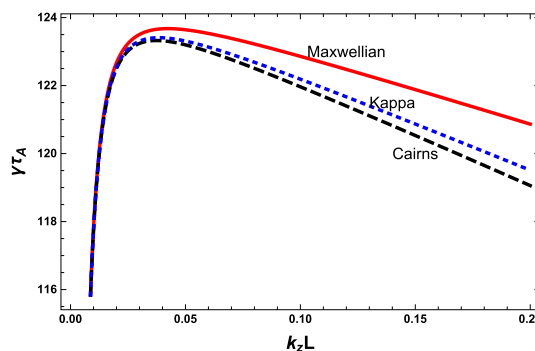

Fig. 1. Variation of the normalized growth rate vs normalized parallel wave number for different distribution of electrons.
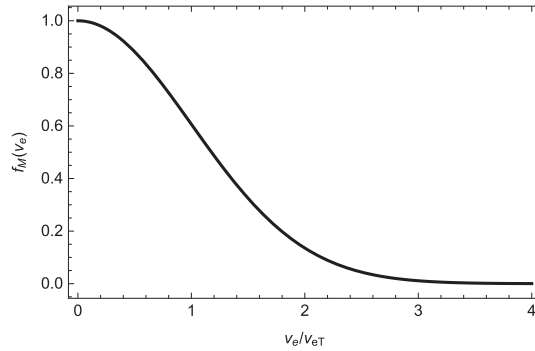
Fig. 2. Plot of Maxwellian distribution function of electrons.

4.1. Resistive drift mode for Maxwellian distribution

Maxwellian distribution of electron can be defined as $f_M(v_e) = (n_e / \pi^{3/2} v_{eT}^3) exp(-v_e^2 / v_{eT}^2)$, where $v_{eT} = (T_e / m_e)^{1/2}$ is the thermal speed of electron and temperature use in energy units which is usual in plasma jargon. Fig. 2 represents the plot of this distribution. It is most probable distribution for electrons under the thermal equilibrium.

By using linear dispersion relation for Maxwell distributed electrons i.e. Eq. (14), it is explored that the real part of the unstable mode follows the Alfven wave dispersion relation $\tilde{\omega} = k_z$, the mode is electromagnetic as shown in Fig. 3 (a). The variation of the normalized imaginary part of the mode against normalized parallel wave
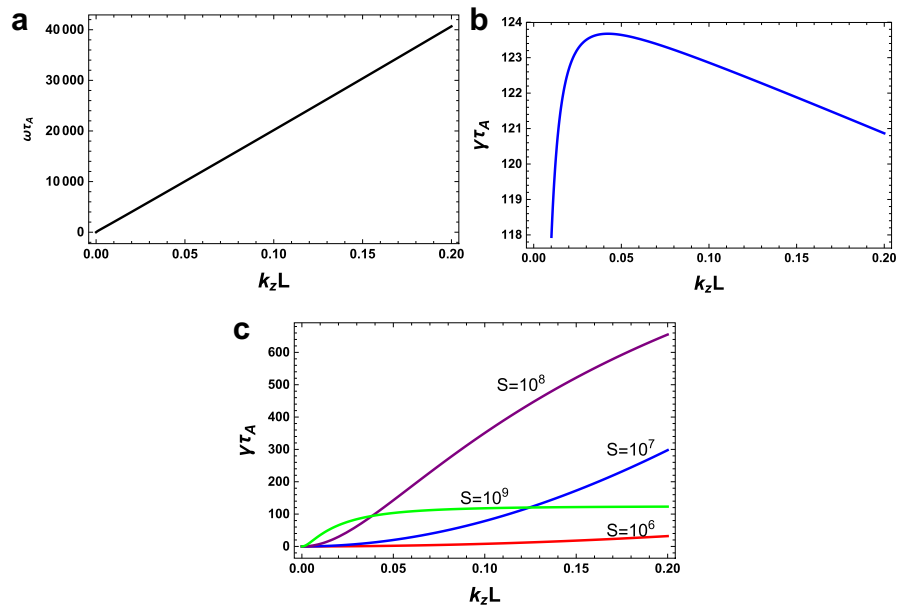

Fig. 3. Plot of dispersion relation (14) for increasing normalized parallel wave number (a) variation of the normalized real part of the mode (b) normalized imaginary part of the mode (c) variation of normalized growth rate for different values of Lundquist number S.
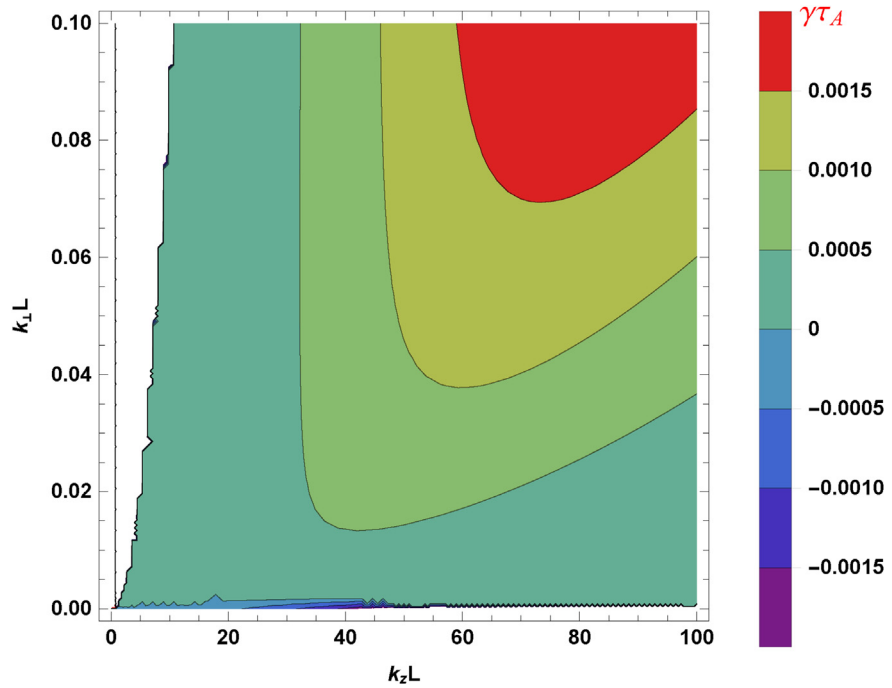
Fig. 4. Contour plot from dispersion relation (14) with parameters $S = 10^7, d_i = 0.1, \beta = 0.5, T_e = 10^5 eV, L_n/L = 2$ and $d_i/L = 0.1$.

number is demonstrated in Fig. 3 (b), whereas Fig. 3 (c) depicted the dependence of the normalized growth rate on normalized parallel wave number for different values of Lundquist number S (usually observed in space plasmas) at $\rho_s k_y \sim 1$.

Fig. 4 is the contour plot of the mode representing the dependence of the normalized growth rate of resistive drift mode on normalized parallel wave number and normalized perpendicular wave number for thermal plasma case.

4.2. Resistive drift mode for Cairns distribution

Cairns distribution of electron can be defined as $f_C(v_e) = (n_e/q_1 \pi^{3/2} v_{eT}^3)(1 + q(v_e^4/v_{eT}^4))exp(-v_e^2/v_{eT}^2)$, where $q_1 = 1 + 3q$ and q estimates the number of thermal
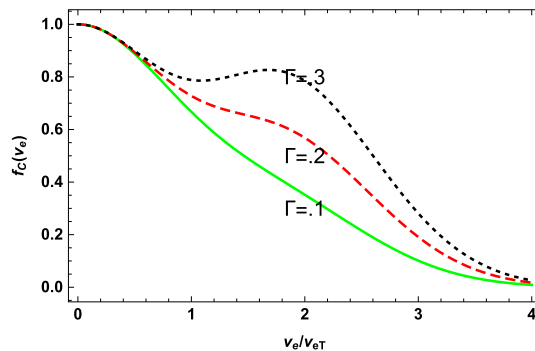

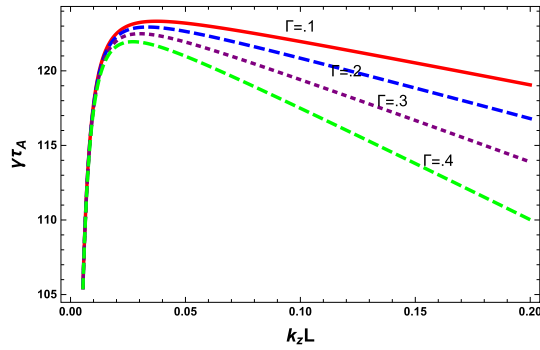**Fig. 5.** Plot of Cairns distribution function of electrons.

Fig. 6. Variation of the normalized growth rate vs normalized parallel wave number for Cairns distributed electrons at different Γ.

electrons. This is the highly non-Maxwellian distribution profile proposed by Cairns et al. [15] which exhibits nonmonotonic attitude in supra-thermal components Fig. 5 represents the plot of this distribution.

Fig. 6 explores the variation of the normalized growth rate of resistive drift mode obtained from linearized Cairns distributed electrons i.e. Eq. (15) for increasing normalized parallel wave number with different values of Γ. It is found that increase the value of Γ decrease the growth rate of the mode hence stabilizing effect on the unstable mode. Furthermore, the growth rate of mode is found lower then Maxwellian distribution case.
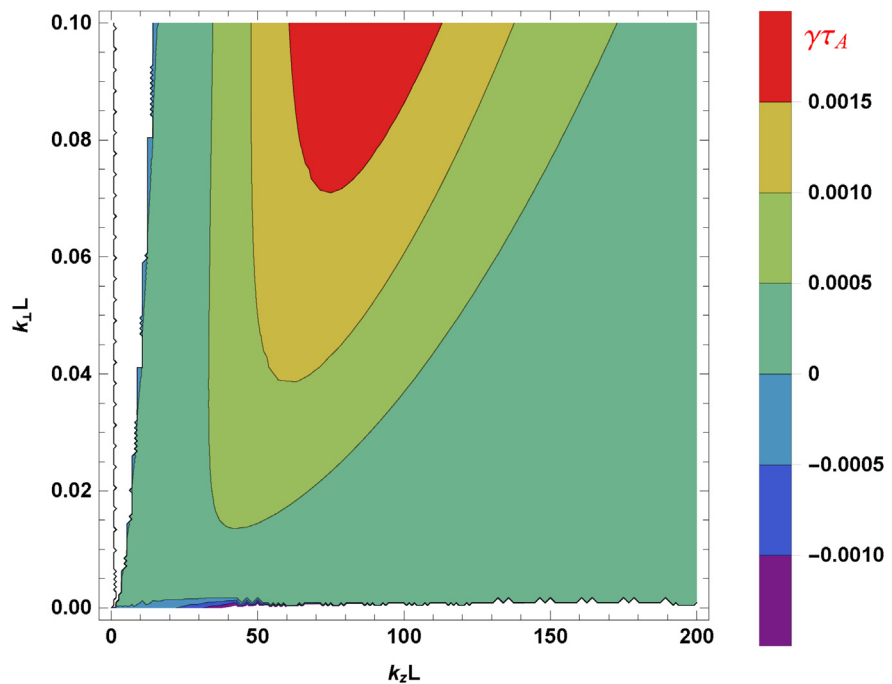

Fig. 7. Contour plot from dispersion relation (15) with parameters $S = 10^7$, $d_i = 0.1$, $\beta = 0.5$, $T_e = 10^5 eV$, $L_n/L = 2$ and $d_i/L = 0.1$.
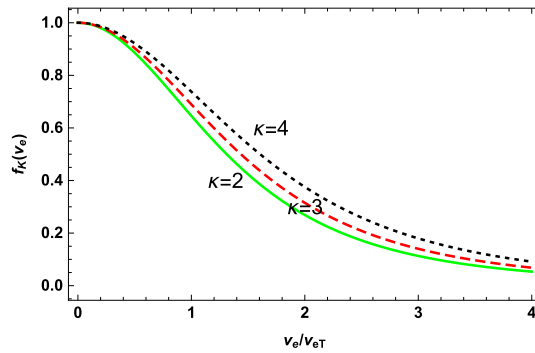
Fig. 8. Plot of kappa distribution function of electrons.

Fig. 7 illustrates the contour plot of the mode represents the dependence of the normalized growth rate of resistive drift mode on normalized parallel wave number and normalized perpendicular wave number for non-thermal i.e. Cairns distributed electron.

4.3. Resistive drift mode for kappa distribution

The kappa distribution of electron can be defined as $f_\kappa(v_e) = (n_e \gamma_\kappa / \pi^{3/2} \kappa_1^2 v_{eT}^3)(1 + (v_e^2 / \kappa \kappa_1^2 v_{eT}^2))^{-(1+\kappa)}$, where $\gamma_\kappa = \gamma(1 + \kappa)/\kappa^{2/3}\Gamma(\kappa - 1/2)$, here γ is the gamma function. This is the commonly used distribution for plasmas that are removed from Maxwellian distribution profile. The kappa distribution has the form of power law and deviates moderately from Maxwellian profile. Fig. 8 represents the kappa distribution profile.

Fig. 9 shows the variation of the normalized growth rate of resistive drift mode obtained from linearized kappa distributed electrons i.e. Eq. (16) for increasing normalized parallel wave number with all other parameters same as Fig. It is found the increasing the spectral index κ for kappa distribution have destabilizing effect on the mode.

Finally, the contour plot for the normalized growth rate against normalized parallel and perpendicular wave number is demonstrated in Fig. 10 by solving Eq. (16)
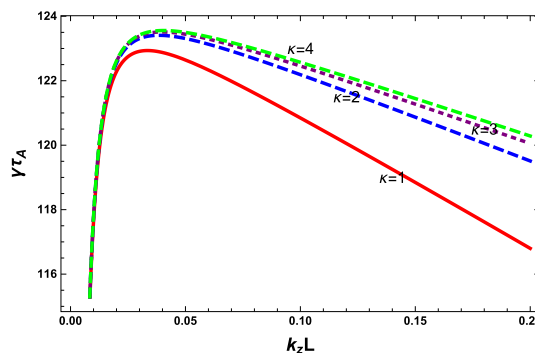

Fig. 9. Variation of the normalized growth rate vs normalized parallel wave vector for kappa distributed electrons at different values of κ.
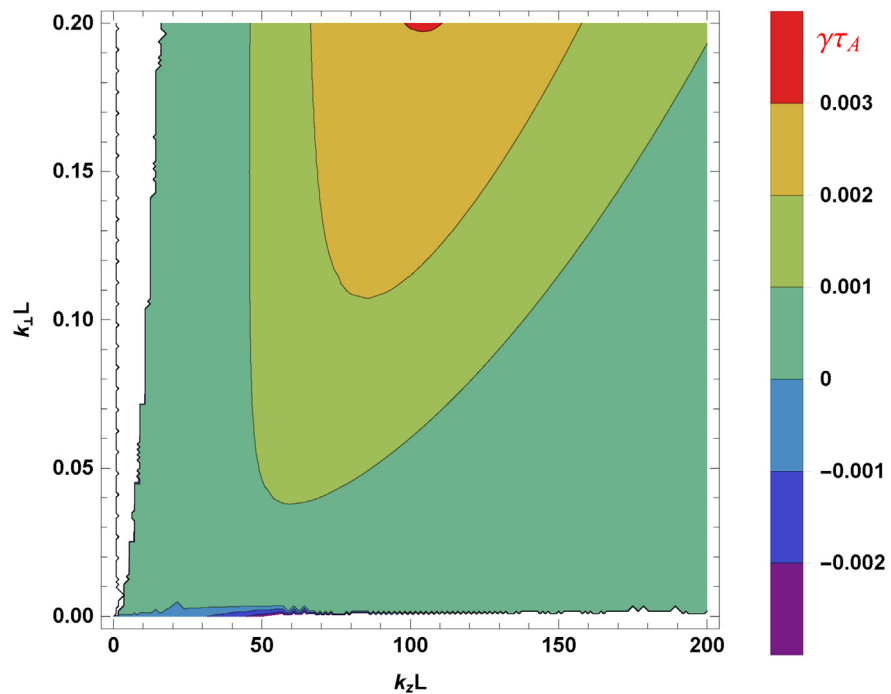
Fig. 10. Contour plot from dispersion relation (15) with parameters $S = 10^7, d_i = 0.1, \beta = 0.5, T_e = 10^5 eV, L_n/L = 2 \ and \ d_i/L = 0.1$.

numerically. Keeping all parameter fixed. It is observed that growth rate is little lower then Maxwellian plasma case.

To summarize, resistive drift instabilities are investigated for thermal as well as non-thermal plasma by using linearize Maxwell-Boltzmann, Cairns and kappa distribution functions. Three dispersion relations for three distributions have been derived. The dispersion relations are then analyzed numerically for typical parameters of space plasma. The growth rate of the unstable mode for thermal and non-thermal plasma is demonstrated. It has been found that increasing values of Γ (which estimate population of non-thermal electrons) for Cairn distributed electrons are able to stabilize the mode. Furthermore, increasing the values of κ (which is spectral index) for the kappa distributed electrons have destabilizing effects on the mode. The present work might be fruitful to understand resistive drift instabilities which are extensively observed in space plasma system.

Declarations

Author contribution statement

Umer Rehman: Conceived and designed the analysis; Analyzed and interpreted the data; Contributed analysis tools or data; Wrote the paper.

Funding statement

Competing interest statement

The authors declare no conflict of interest.

Additional information

No additional information is available for this paper.

References

[1] S.S. Moiseev, R. Z Sagdeev, Effect of finite electrical conductivity on the stability of a plasma confined by a magnetic field, Zh. Tekh. Fiz. 34 (1964) 248. [S. S. Moiseev, and R. Z Sagdeev (1964), Soviet- Physics-Technical Physics. 9, 196.].

[2] A.B. Mikhailovskii, Drift wave stability under linear theta-pinch conditions, Nucl. Fusion 12 (1972) 55.

[3] A.B. Mikhailovskii, Electromagnetic Instabilities in an Inhomogeneous Plasma (Atomizdat, Moscow, 1971), IOP, Bristol, Ebook, 1992.

[4] V.V. Mirnov, J.P. Sauppe, C.C. Hegna, C.R. Sovinec, Analytical and numerical treatment of resistive drift instability in a plasma slab, Plasma Phys. Rep. 42 (2016) 5.

[5] W.C. Feldman, J.R. Asbridge, S.J. Bame, M.D. Montgomery, Double ion streams in the solar wind, J. Geophys. Res. 78 (1973) 2017.

[6] V. Formisano, P.C. Hedgecock, Solar wind interaction with the Earth's magnetic field: 3. On the Earth's bow shock structure, J. Geophys. Res. 78 (1973) 3745.

[7] J.D. Scudder, E.C. Sittler Jr., H.S. Bridge, A survey of the plasma electron environment of Jupiter: a view from Voyager, J. Geophys. Res. 86 (1981) 8157.

[8] E. Marsch, K.H. Mahlhauser, R. Schwenn, H. Rosenbauer, W. Pilipp, F.M. Neubauer, Solar wind protons: three-dimensional velocity distributions and derived plasma parameters measured between 0.3 and 1 AU, J. Geophys. Res. 87 (1982) 52.

[9] J.T. Gosling, J.R. Asbridge, S.J. Bame, W.C. Feldman, Solar wind stream interfaces, J. Geophys. Res. 83 (1981) 1401.

[10] R.P. Lin, W.K. Levedahl, W. Lotko, D.A. Gurnett, F.L. Scarf, Evidence for nonlinear wave-wave interactions in solar type III radio bursts, Astrophys. J. 308 (1986) 954.

[11] R.E. Ergun, D. Larson, R.P. Lin, et al., Wind spacecraft observations of solar impulsive electron events associated with solar type III radio bursts, Astrophys. J. 503 (1998) 435.

[12] D.A. Whelan, R.L. Stenzel, Electromagnetic radiation and nonlinear energy flow in an electron beam-plasma system, Phys. Fluids 28 (1985) 968.

[13] R.J. Fitzenreiter, K.W. Ogilvie, D.J. Chornay, J. Keller, Observations of electron velocity distribution functions in the solar wind by the WIND spacecraft: high angular resolution strahl measurements, Geophys. Res. Lett. 25 (1998) 249.

[14] V.M. Vasyliunas, A survey of low-energy electrons in the evening sector of the magnetosphere with OGO 1 and OGO 3, J. Geophys. Res. 73 (1968) 2839.

[15] R.A. Cairns, A.A. Mamum, R. Bingham, R. Bostrom, R.O. Dendy, C.M.C. Naim, P.K. Shukla, Electrostatic solitary structures in non-thermal plasmas, Geophys. Res. Lett. 22 (1995) 2709.

[16] S.P. Christon, D.G. Mitchell, D.J. Williams, L.A. Frank, C.Y. Huang, T.E. Eastman, Energy spectra of plasma sheet ions and electrons from ~ 50 eV/e to ~ 1 MeV during plasma temperature transitions, J. Geophys. Res. 93 (1988) 2562.

[17] R. Smets, D. Delcourt, D. Fontaine, Ion and electron distribution functions in the distant magnetotail: modeling of Geotail observations, J. Geophys. Res. 103 (1998) 20407.

[18] A.T.Y. Lui, Parameter extraction of source plasma from observed particle velocity distribution, Geophys. Res. Lett. 33 (2006) L21108.

[19] R. Bostrom, Observations of weak double layers on auroral field lines, IEEE Trans. Plasma Sci. 20 (1992) 756.

[20] P.O. Dovner, A.I. Eriksson, R. Bostrom, B. Holback, Freja multiprobe observations of electrostatic solitary structures, Geophys. Res. Lett. 21 (1994) 1827.

[21] A.A. Mamun, Effects of ion temperature on electrostatic solitary structures in nonthermal plasmas, Phys. Rev. E 55 (1997) 1852.

[22] T.K. Baluku, M.A. Hellberg, Dust acoustic solitons in plasmas with kappa-distributed electrons and/or ions, Phys. Plasmas 15 (2008) 123705.

[23] E.E. Antonova, N.O. Ermakova, Kappa distribution functions and the main properties of auroral particle acceleration, Adv. Space Res. 42 (2008) 987.

[24] S.A. Khan, A. Rehman, J.T. Mendonca, Kinetic study of ion-acoustic plasma vortices, Phys. Plasmas 21 (2014), 092109.

[25] A. Rehman, S.A. Shan, M.Y. Hamza, J.K. Lee, Effect of orbital angular momentum on electron acoustic waves in double-Kappa plasma, J. Geophys. Res. Space Phys. 122 (2017) 1690.

[26] M. Usman Malik, W. Masood, A.A. Mirza, Unique features of parallel whistler instability in a plasma with anisotropic Cairns distribution, Phys. Plasmas 24 (2017) 102120.

[27] N. Batool, W. Masood, A.A. Mirza, The effects of nonthermal electron distributions on ion-temperature-gradient driven drift-wave instabilities in electron-ion plasma, Phys. Plasmas 19 (2012), 082111.

[28] H.L. Pecseli, Series in Plasma Physics: Waves and Oscillations in Plasmas, CRC Press, 2013.